Solid State Electronics 149 (2018) 15–22

Contents lists available at ScienceDirect

Solid State Electronics

journal homepage: www.elsevier.com/locate/sse

Analyses of current-voltage characteristics using derivative methodology

Wei-Fu Wang[a,*], Kai-Yuan Cheng[a], Meng-Chyi Wu[a], Kuang-Chien Hsieh[a,b]

[a] Institute of Electronic Engineering, National Tsing Hua University, Hsinchu 30013, Taiwan
[b] Center for Nanotechnology, Materials Science and Microsystems, National Tsing Hua University, Hsinchu 30013, Taiwan

ARTICLE INFO

The review of this paper was arranged by Prof. S. Cristoloveanu

Keywords:
Diode model
Norde plot
Ideality factor
Parasitic resistance
Turn-on voltage

ABSTRACT

An alternative methodology to the modified Norde's model is presented to determine both series and shunt parasitic resistance, ideality factor and the resistance-mediated "turn-on" voltage of diodes by measuring derivatives of I-V characteristics. Experimental results follow to support the theoretical investigation and demonstrate a self-consistency check.

1. Introduction

p-n junction diodes or Schottky diodes are known for their rectifying characteristics. Current-voltage and capacitance-voltage measurements are important tools used to characterize diodes [1,2]. Norde [3] in 1979 and many others [4–6] since then have used modified I-V plots to determine the ideality factor and barrier height of Schottky diodes even if associated with high series resistance. On the other hand, the forward diode current increases sharply above the so-called "turn-on" or "knee" voltage, generally estimated by the tangent intercept approach or simply defined at which a certain current is reached. In this work, we expand on Norde's model and present a methodology based on derivatives of I-V characteristics to determine the actually resistance-mediated "turn-on" voltage, parasitic resistance and ideality factor for both junction and Schottky diodes. This long-overlooked derivative I-V technique (DIV) supported with experimental data is shown versatile and informative.

2. I-V characteristics and its derivatives

In theory, the ideal diode current increases exponentially upon forward biasing and the differential resistance of the junction reduces quickly to become negligible compared to the parasitic resistance in the measurement system. Fig. 1 is a schematic diagram of a current-voltage relationship of either p/n junction or Schottky diodes. The difference between theory and measurement comes from the parasitic resistance associated with the quasi-neutral region, and contact resistance, shunt leakage and system resistance of the measurement equipment, denoted as R_{sub}, R_p, and R_s respectively.

As shown in the inset of Fig. 1, only the fraction V_j drops across the depletion region for a given voltage V applied by the power supply. A voltage difference of $IR_s + I_jR_{sub}$ is still needed to drive the current through the circuit. The current has a negligible rising slope with respect to voltage at small bias and also a nearly constant slope at large bias suggesting that a peak of the second derivative forms in between with the first derivative going through an inflection point at the voltage peak as shown in Fig. 1.

It is generally accepted that the junction current increases as $I_j = I_{js}[e^{qVj/nkT} - 1]$ with the voltage drop V_j across the junction depletion region, where I_{js} is the reverse saturation current and n the ideality factor. It is easy to find the differential conductance of the junction to be $dI_j/dV_j = I_j/nV_T$, where $V_T = kT/q$, the thermal voltage. Its inverse is the differential junction resistance. To proceed with further analysis on the I-V relationship we have four different combinations among resistances from quasi-neutral region (including the contact resistance), leakage and measurement system, i.e. R_{sub}, R_p and R_s.

2.1. Negligible leakage $G_p = 1/R_p = 0$ and negligible substrate/contact resistance ($R_{sub} = 0$)

Most I-V models assume that the overall resistance of a diode consists only the junction differential resistance R_j and a parasitic series resistance R_s, i.e. Switch S_{sub} is shorted while S_p is open, and the following relationships hold assuming R_s is a constant.

* Corresponding author.
E-mail address: s101063703@m101.nthu.edu.tw (W.-F. Wang).

https://doi.org/10.1016/j.sse.2018.08.002
Received 10 April 2018; Received in revised form 20 July 2018; Accepted 3 August 2018
Available online 10 August 2018

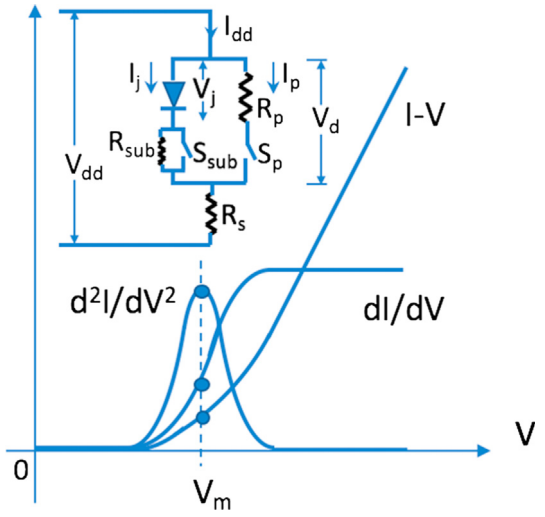

Fig. 1. A schematic diagram of current-voltage dependence of diodes; Junction current increases exponentially in theory but at large forward bias the current is eventually restricted by the parasitic resistance including the bulk substrate resistance and contact resistance, denoted as R_{sub}, and the load resistance in the measurement equipment, indicated as R_s in the inset. The shunt leakage is shown with an equivalent shunt resistance, R_p. When the shunt resistance is much greater than the series resistance, a simplified result is realized so that all the series resistances can be lumped together to become a single term of R_s. Also shown are corresponding diagrams of the first and second derivatives of the I-V dependence. A peak appears in the second derivative at voltage V_m and dots mark the numerical values of current, first derivative and second derivative at V_m, respectively.

$$\frac{dI}{dV} = \frac{1}{R_s + R_j} = \frac{1}{R_s + \frac{nV_T}{I_j}} = \frac{1}{R_s + \frac{nV_T}{I}} \tag{1}$$

$$\frac{d^2I}{dV^2} = \frac{dI}{dV} * \frac{nV_T}{(IR_s + nV_T)^2} \tag{2}$$

Assuming the second derivative has a differentiable peak, the slope around the peak voltage would be zero. We set the derivative of the second derivative (Eq. (2)) to be zero at the voltage peak, V_m, i.e. $d[d^2I/dV^2]/dV = 0$ at $V = V_m$ and $I = I_m$. Going through the differentiation process and equating both sides, we get the following results of Eqs. (3)–(5). The identification of the peak at V_m along the second derivative curve allows one to determine the numerical values of I_m, and $1/R_m$ and Q_m of both first and second derivatives as marked in Fig. 1, respectively, sufficient to solve Eqs. (3), (4) and (5). It becomes straight forward to determine the ideality factor and series resistance using the derivative technique and compare the conventionally tangent-defined turn-on voltage with the peak voltage V_m.

$$2I_m R_s = nV_T \tag{3}$$

$$\frac{1}{R_m} = \frac{dI}{dV}_{V_m, I_m} = \frac{1}{3R_s} \tag{4}$$

$$Q_m = \frac{d^2I}{dV^2}_{V_m, I_m} = \frac{4}{27nR_s V_T} \tag{5}$$

2.2. Non-negligible leakage $G_p = 1/R_p \neq 0$ but negligible substrate/contact resistance ($R_{sub} = 0$)

For some diodes, leakage between cathodes and anodes through surface is not necessarily negligible, particularly when improperly passivated. In this case, R_p is not necessarily infinity, i.e. both Switch S_{sub} and S_p are closed. The equivalent junction resistance is $R_j = nV_T/I_j = nV_T/(I - I_p) = nV_T/[I(R_p + R_s)/R_p - V/R_p]$. Assuming that both R_s and R_p are constants independent of voltage, one can find the following relationships on first and second derivatives. Be borne in mind that the measured current I is the sum of both junction current I_j and leakage current I_p.

$$\frac{dI}{dV} = \frac{1}{R_s + \frac{R_j R_p}{R_j + R_p}} \tag{1′}$$

$$\frac{d^2I}{dV^2} = \frac{dR_j}{dV} * \frac{-R_p^2}{[R_j(R_s + R_p) + R_s R_p]^2} \tag{2′}$$

Assuming the second derivative has a differentiable peak, the slope around the peak voltage would be zero. Setting the derivative of the second derivative (Eq. (2′)) to be zero at the voltage peak, V_m, i.e. $d[d^2I/dV^2]/dV = 0$ at $V = V_m$ and $I = I_m$ and going through the differentiation process and equating both sides, we get the following results.

$$2I_{jm}R_s = 2\left[\left(1 + \frac{R_s}{R_p}\right)I_m - \frac{V_m}{R_p}\right]R_s = nV_T \tag{3′}$$

$$\frac{1}{R_m} = \frac{dI}{dV}_{V_m, I_m} = \frac{R_p + 2R_s}{3R_s R_p + 2R_s^2} \tag{4′}$$

$$Q_m = \frac{d^2I}{dV^2}_{V_m, I_m} = \frac{4R_p^3}{R_s(3R_p + 2R_s)^3 nV_T} \tag{5′}$$

The identification of the peak at V_m along the second derivative curve allows one to determine the numerical values of I_m, and $1/R_m$ and Q_m of both first and second derivatives as marked in Fig. 1, respectively, sufficient to solve Eqs. (3′), (4′) and (5′). By substituting Eq. (3′) for nV_T in Eq. (5′) and eliminating R_p in terms of R_s through Eq. (4′), $R_p = 2R_s(R_m - R_s)/(3R_s - R_m)$, we then derive the following higher-degree polynomial relationship with which R_s can be solved numerically. While $R_s < R_m < 3R_s$, R_s is usually slightly larger than one third of R_m for low leakage i.e. $1/R_p$ being negligible.

$$(R_m - R_s)^4 = 2Q_m R_s(I_m R_s^2 + I_m R_m R_s - 3V_m R_s + V_m R_m) \tag{6′}$$

Once R_s is computed, it then becomes straight forward to determine R_p, and ideality factor n, where $R_p = 2R_m(R_m - R_s)/(3R_s - R_m)$ and $n = [V_m R_m + (I_m R_m - 3V_m)R_s + I_m R_s^2]/[(R_m - R_s)V_T]$.

2.3. Neither negligible substrate/contact resistance ($R_{sub} \neq 0$) nor negligible leakage current ($G_p \neq 0$)

As the device processing complexity goes one step up, some diodes are fabricated in a quasi-vertical structure and the substrate resistance associated with the quasi-neutral region may not be negligible any more, i.e. Switch S_{sub} is open while S_p is closed. Also, ideal ohmic contacts are often hard to make for high band-gap semiconductors or lightly doped materials or when large-area Schottky contacts are used as contacts resulting in high contact resistance. In these cases, R_{sub} needs to be included in the overall resistance.

$$\frac{dI}{dV} = \frac{1}{R_s + \frac{(R_{sub} + R_j)R_p}{R_{sub} + R_j + R_p}} \tag{1″}$$

$$\frac{d^2I}{dV^2} = \frac{dR_j}{dV} * \frac{-R_p^2}{[R_j(R_s + R_p) + (R_s R_{sub} + R_{sub} R_p + R_s R_p)]^2} \tag{2″}$$

Assuming the second derivative has a differentiable peak again, the slope around the peak voltage would be zero. Setting the derivative of the second derivative (Eq. (2″)) to be zero at the voltage peak, V_m, i.e. $d[d^2I/dV^2]/dV = 0$ at $V = V_m$ and $I = I_m$ and going through a lengthy differentiation process and equating both sides, we get the following results.

$$2I_{jm} = 2\left[\left(1 + \frac{R_s}{R_p}\right)I_m - \frac{V_m}{R_p}\right] = nV_T \frac{R_p + R_{sub}}{R_s R_{sub} + R_{sub} R_p + R_s R_p} \tag{3″}$$

$$\frac{1}{R_m} = \frac{dI}{dV}_{V_m,I_m} = \frac{(R_p + R_{sub})^2 + 2(R_sR_{sub} + R_{sub}R_p + R_sR_p)}{(3R_p + 2R_s + R_{sub})(R_sR_{sub} + R_{sub}R_p + R_sR_p)} \quad (4'')$$

$$Q_m = \frac{d^2I}{dV^2}_{V_m,I_m} = \frac{4{R_p}^3(R_p + R_{sub})}{(3R_p + 2R_s + R_{sub})^3(R_sR_{sub} + R_{sub}R_p + R_sR_p)nV_T} \quad (5'')$$

Unfortunately, we fall short by one more measurable quantity to determine all four unknowns of R_{sub}, R_p, R_s and ideality factor n since the identification of the peak at V_m along the second derivative curve only gives the numerical values of I_m, and $1/R_m$ and Q_m of both first and second derivatives as marked in Fig. 1. To seek the fourth relationship among R_{sub}, R_p, R_s and n, yet independent of the derivative approach, we turn to the Norde plot.

It is clear from Fig. 1 that $V_d = V - IR_s$ and $I = I_j + I_p$. Taking into account the dependence of diode junction current on the voltage drop across the depletion region, V_j, we obtain the following relationship, where I_{js} is the reverse saturation current.

$$I = I_{js}(e^{V_{j/nV_T}} - 1) + I_p \cong I_{js}(e^{V_{j/nV_T}}) + I_p = I_{js}\left(e^{\left[V - IR_s - IR_{sub} + \frac{R_{sub}}{R_p}(V - IR_s)\right]/nV_T}\right) + \frac{V - IR_s}{R_p}$$

$$\frac{dI}{dV} = \frac{\frac{1}{R_p} + \frac{I}{nV_T}\left(1 + \frac{R_{sub}}{R_p}\right)}{1 + \frac{R_s}{R_p} + \frac{I}{nV_T}\left(R_s + R_{sub} + \frac{R_sR_{sub}}{R_p}\right)}$$

We then define F(V) which is slightly different from Norde's original function by replacing the effective Richardson constant with the reverse saturation current directly. In addition, we neglect the leakage current I_p from I since I_p is usually small. The error induced by neglecting I_p may be insignificant but it needs to be validated later.

$$F(V) \equiv \gamma V - V_T \ln\frac{I}{I_{js}} = \left[\gamma - \frac{1}{n} - \frac{R_{sub}}{nR_p}\right]V + \frac{I\left(R_s + R_{sub} + \frac{R_sR_{sub}}{R_p}\right)}{n} \quad (6'')$$

For small current I, F(V) decreases with V approximately with a negative slope of $\gamma - \frac{1}{n} < 0$ by choosing $\gamma < \frac{1}{n}$. On the other hand, for very large current where the diode current is dominated by parasitic resistance so that I is proportional to V, the γV term in Eq. (6″) is proportional to I and the ln(I/I_{js}) term would then be negligible since $x > \ln(x)$ for large x. Consequently, F(V) increase with V with a slope γ which is positive. Therefore, F(V) goes through a minimum as V varies and we expect dF/dV = 0 at the local minimum, V_o and the current I_o can be readily read off the I-V curve. Setting dF/dV = 0 at V_o, we then obtain two measurable quantities.

$$I_o\gamma\left[R_s + R_{sub}\left(1 + \frac{R_s}{R_p}\right)\right] = V_T\left[1 - n\gamma\left(1 + \frac{R_s}{R_p}\right)\right] \quad (7'')$$

$$F(V_o) = \left(\gamma - \frac{1}{n} - \frac{R_{sub}}{nR_p}\right)V_o + \frac{I_o\left(R_s + R_{sub} + \frac{R_sR_{sub}}{R_p}\right)}{n} \quad (8'')$$

Although it is doable, it is not trivial to solve all R_{sub}, R_p, R_s and n using Eqs. (3″) to (5″) and (7″) since it involves solving high-degree nonlinear functions. An iteration process of numerical analysis is recommended as follows. First, go through Eqs. (3′) to (6′) to find R_s, R_p and n for any set of carefully performed I-V measurements assuming a starting value of $R_{sub} = 0$. Then construct the modified Norde plot with an appropriate value of $\gamma = 1/2$, for example. Identify the voltage minimum in the Norde plot and obtain the corresponding current I_o before finding R_{sub} using Eq. (7″) with the new finding of R_s, R_p and n from the DIV technique. Having a correction term of R_{sub} we can proceed with Eqs. (3″) to (5″) to find a new round of R_s, R_p and n before finding a new correction of R_{sub} using Eq. (7″) again. Repeat the iteration process until an acceptable error is met, i.e. all data of R_{sub}, R_s, R_p, and n converge self-consistently. However, in the iteration process with each newly measured R_{sub} correction, we need to substitute Eq. (3″)) for Eq. (5″) and eliminate R_p in terms of R_s and R_{sub} through Eq. (4″) before we derive and solve a high-degree polynomial of R_s numerically. The relationship among R_p, R_s and R_{sub} is found by solving the quadratic equation of R_p by expanding Eq. (4″) and consolidating items of the same order as shown in the Appendix.

2.4. Degenerate case of 2.3 when shunt leakage is non-negligible ($G_p \neq 0$) but R_s is negligible as compared to R_{sub} and R_p

From the circuit modeling point of view, a degenerate case of Case 2.3 may form when the effect of R_s is negligible as compared to the resultant resistance due to the shunt leakage and substrate/contact resistance. A technical example would consist concentric rings of top-contact Schottky diodes. The inner circle acts as the normal Schottky junction while the much larger reverse-biased outer ring serves as a quasi-ohmic contact. A shunt leakage may exist between the two separated but poorly passivated rings. The leakage shunts directly from one metal electrode to the other bypassing the substrate and contact resistance ($R_{sub} + R_{cont}$) and the minor resistance associated with the measurement system ($R_s \sim 0$) could then be neglected. In this scenario,

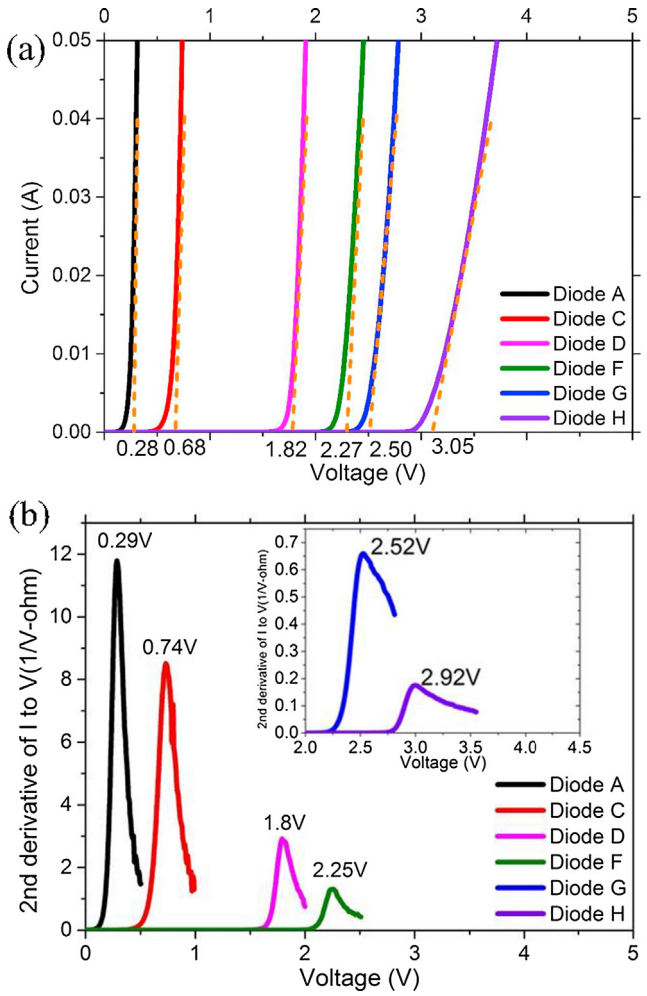

Fig. 2. I-V characteristics of various diodes; the current compliance is set at 0.05 A to minimize the rise of junction temperature and to protect the measurement system. (a) Dash-line tangents are drawn to show different voltage intercepts and the turn-on voltages by the linear fit approach. (b) Corresponding peaks in the second derivative of I-V curves. The inset is plotted for Diodes G and H in an enlarged vertical scale in unit of 1/V-ohm.

the corresponding current-voltage relationships can be found as follows.

$$\frac{dI}{dV} = \frac{1}{\frac{(R_{sub}+Rj)R_p}{R_{sub}+R_j+R_p}} \quad (1''')$$

$$\frac{d^2I}{dV^2} = \frac{dR_j}{dV} * \frac{-{R_p}^2}{[R_jR_p + R_{sub}R_p]^2} \quad (2''')$$

Again, assuming that the second derivative has a peak, the third derivative at the voltage V_m would be zero. In other words, $d[d^2I/dV^2]/dV = 0$ at $V = V_m$ and $I = I_m$ and the following results are obtained.

$$2I_{jm} = 2\left[I_m - \frac{V_m}{R_p}\right] \quad (3''')$$

$$\frac{1}{R_m} = \frac{dI}{dV_{V_m,I_m}} = \frac{(R_p + R_{sub})^2 + 2R_{sub}R_p}{R_{sub}R_p(3R_p + R_{sub})} \quad (4''')$$

$$Q_m = \frac{d^2I}{dV^2{}_{V_m,I_m}} = \frac{4{R_p}^3(R_p + R_{sub})}{R_{sub}R_pnV_T(3R_p + R_{sub})^3} \quad (5''')$$

From Eq. (4‴) R_p can be expressed in terms of R_m and R_{sub}, and

$$R_p = \frac{R_{sub}\left[-(4R_m - R_{sub}) - \sqrt{12{R_m}^2 + 4R_mR_{sub} + {R_{sub}}^2}\right]}{2(R_m - 3R_{sub})} \quad (6''')$$

Two Eqs. (5‴) and (6‴) are sufficient to solve two unknowns, R_{sub} and R_p. R_{sub} can be numerically solved after substituting Eq. (6‴) in Eq. (5‴)) and eliminating R_p in terms of R_{sub}.

3. Experimental results

3.1. Comparison of turn-on voltages

To test our hypothesis we have measured commercial and lab-made diodes assuming first the shunt leakage and substrate resistance are negligible. Fig. 2 shows the I-V characteristics with a current compliance set at 0.05 A to minimize the rise of junction temperature and to protect the measurement system, Keithley 2400. The turn-on voltages covering a wide range from 0.3 V to above 3 V determined by the conventional tangent intercept and the second derivative approach are listed in Table 1. Included are ideality factors determined from Eqs. (3)–(5). First of all, all I-V curves have local maxima in the corresponding second derivatives as expected in the abovementioned derivation of equations, and the peak positions are close to the tangent intercept ones. It seems feasible to use the derivative technique as an alternative approach to determine the turn-on or knee voltages of diodes.

It is worthy to note that this DIV technique provides a self-check about the measurement consistency at least for the case when both shunt leakage and substrate resistance are negligible. In this case, ratio of the measured results of Eqs. (4) and (5) (i.e. Eq. (4)/Eq. (5)) can be coupled back to Eq. (3) to yield I_m, which can also be read directly from the I-V results. The difference between the calculated and read-off I_m tells the deviation. The second to last column of Table 1 lists the self-consistency check of I-V measurement of each diode. Since derivative and higher order derivatives are very sensitive mechanisms to kinks and irregularities along any function. Coarse I-V measurements with large voltage steps may easily lead to inaccurate determination of derivatives. The recommended methodology is to apply coarse measurements first to quickly identify the approximate positions of V_m, and then fine-tune I-V measurements in the vicinity of the approximate V_m with much smaller voltage steps. It is found a refined I-V can greatly improve the measurement deviation to better than 10%. On the other hand, a large error may also suggest a deficiency of this simplified model and correction with non-negligible shunt leakage and substrate resistance is indeed necessary.

3.2. Comparison with Norde model and resistance effect

Norde [3] used modified plot of I-V, defined as F(V), to determine Schottky barrier heights of diodes having large series resistance. Numerous plots of F(V) can be chosen by varying the slope constant [4], γ. For diodes with a simple ideality factor n = 1, the expected product of the measured current and series resistance equals thermal voltage, i.e. $I_oR_o = V_T$ according to Norde's initial choice of slope constant being 1/2. The current-resistance product is actually twice as large as Eq. (3) in our model suggesting our measured current is one half that of the Norde method for a slope constant of 1/2. We expect a different slope constant of 2/3 in the Norde plot can bring these two models coinciding, i.e. the voltage maximum in our model matching with the voltage minimum in the Norde plot. Fig. 3 shows I-V measurements of the Si Schottky diode, Diode A, 1N5817 in Table 1. The diode has been intentionally

Table 1
Results of ideality factor and parasitic resistance of diodes and comparison of turn-on voltages determined with the conventional tangent intercept approach and second derivative of I-V characteristics.

	V_m (V)[a]	V_t (V)[b]	$1/R_s$ (measured)[c]	dI/dV[d]	d^2I/dV^2 [e]	I_m (mA)[f]	I_m-cal (mA)[g]	Deviation (%)[h]	n (ideality factor)[i]
Diode A	0.29	0.28	2.06	0.688	11.80	26.96	26.74	−0.81	1.00
Diode B	0.33	0.33	0.26	0.088	1.47	3.51	3.48	−0.88	1.02
Diode C	0.74	0.68	2.37	0.791	8.36	49.8	49.89	0.19	1.62
Diode D	1.80	1.82	0.58	0.194	2.91	9.13	8.58	−6.35	1.14
Diode E	1.92	1.97	0.10	0.034	0.31	2.63	2.52	−4.43	1.91
Diode F	2.25	2.27	0.34	0.113	1.31	6.32	6.49	2.65	1.48
Diode G	2.52	2.50	0.20	0.067	0.66	4.66	4.49	−3.88	1.73
Diode H	2.99	3.05	0.05	0.018	0.18	1.13	1.16	2.82	1.71
Diode I	0.32	0.36	7.13E−03	2.38E−03	2.89E−02	0.132	0.130	−1.43	1.41
Diode J	0.14	0.15	3.98E−03	1.33E−03	2.26E−02	0.047	0.052	3.89	1.01

Diode A: Si Schottky 1N5817, Micro-commercial components; Diode B: Ge diode, 1N60P, Taitron; Diode C: Si p/n 10N10, Rectron semiconductor; Diode D: InGaP red LED LS-1W/GH-URC, Centenary Materials; Diode E: GaP LED LS-F3UGC-YBL, Centenary Materials; Diode F: InGaN green LED LS-1W/GH-UPGC, Centenary Materials; Diode G: InGaN blue LED LS-1W/GH-UBC, Centenary Materials; Diode H: InGaN purple LED 3RS4VCS, Centenary Materials. Diode I and Diode J are made in the lab by evaporating Schottky Al contacts on p-type GaAs and Si, respectively.

[a] V_m indicates the voltage of the peak in the second derivative.

[b] V_t denotes the voltage intercept from the linear fitting of I-V curve.

[c] R_s means the series resistance calculated according to Eq. (3), in the unit of ohm.

[d] dI/dV and [e] d^2I/dV^2 are values of the first and second derivative at V_m, respectively (in the unit of S and S/V).

[f] I_m indicates the read-off current at V_m, while [g] I_m-cal is the current calculated and can be compared with I_m, therefore the [h] Deviation between theoretical and the read-off value can be estimated.

[i] n here denotes the calculated ideality factor of the diode.

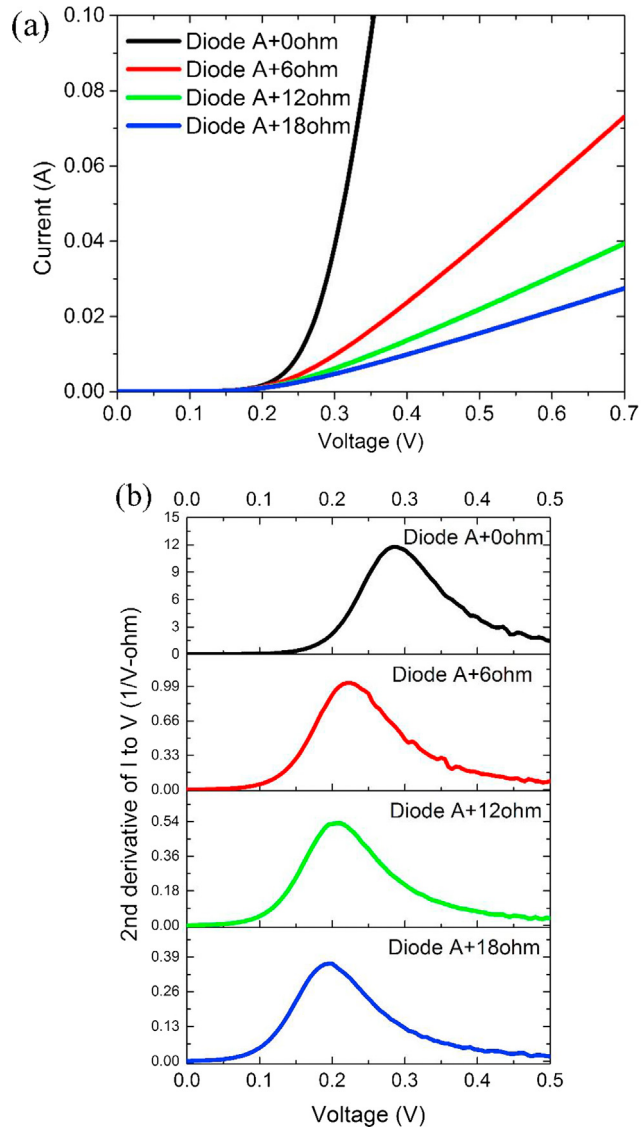

Fig. 3. Effect of series resistance on (a) the I-V dependence and (b) second derivatives of Diode A, Schottky diode 1N5817 from Micro-commercial components. As the series resistance increases, the peak position of the second derivative moves to lower voltage and peak height reduces.

connected with additional external resistance having nominal values of 6, 12 and 18O. The detailed numerical values of current, voltage, first and second derivatives are listed in Table 2. As the net resistance increases with added external resistance, the measured current reduces for a given supplied voltage. The second derivative peaks move progressively toward lower voltages as well, similar to the trend found by the tangent intercept approach. The ideality factors for these four sets of I-V measurements are fairly close to 1 so the corresponding voltages dropped across the depletion region can be easily found using $V_{jm} = V_m - \frac{1}{2} nV_T$ for the measurement temperature at 25 °C. Consequently, the corresponding reverse saturation current for each setting can be calculated with $I_m = I_s [\exp(V_{jm}/nV_T) - 1]$, and the average of all four settings is found to be 6.89×10^{-7} A with a relative error of ± 4%. The small percentage of error shows self-consistency of the DIV model. More importantly, these results can be compared with those obtained with the Norde plots. It is fortunate that the voltage minimum can still be determined without knowing the exact dimensions of the diode cross section which are critical to determining the Schottky barrier height. The corresponding Norde plot of Diode A for each combination with an external series resistance gives rise to a voltage minimum for a slope constant of 2/3 and the measured voltage minima are in close agreement with the voltage maxima measured in the DIV approach as listed also in Table 2. The important result obtained by comparing the two models is that the DIV approach matches with a special case of the Norde plot for a specific slope constant. Yet, the Norde approach provides additional measurable quantities complementary to the DIV approach when incorporation of shunt leakage and substrate resistance in diode modeling is needed.

One particular point worthy to note is about the decreasing voltage of derivative maximum with increasing parasitic resistance. From that perspective, the meaning of conventional terminology of “turn-on” voltage can be misleading. It is awkward to comprehend a device that would turn on at smaller voltages with increasing resistance instead of decreasing resistance. As seen from Eq. (3), the voltage maximum is the voltage at which the product of diode current and series resistance equals $\frac{1}{2} nV_T$. It is actually a resistance-mediated voltage. All things being equal except impurity doping concentration, a p/n junction having a larger contact potential would have smaller reverse saturation current and smaller series resistance, and it would require a larger junction voltage to inject current to meet Eq. (3) i.e. requiring a larger turn-on voltage so to speak. Without knowing detailed device structure and processing conditions, it would be generally difficult to compare “turn-on” voltages of diodes even of the same kinds, however. In addition, Eq. (4) indicates that at this resistance-mediated voltage the overall circuit resistance is three times diode series resistance. Equivalently speaking, the junction resistance associated with the depletion region is twice as large as the diode series resistance at this particularly supplied voltage, beyond which the junction resistance would soon become smaller than the series resistance consisting of substrate resistance, contact resistance and measurement system resistance.

3.3. Effect of shunt leakage and substrate resistance

Werner [7] has investigated the effect of shunt resistance on I-V measurements of p/n or Schottky diodes, which contributes to the leakage current. The measured reverse bias current was used to estimate the shunt conductance and an over-estimated correction current of shunt conductance multiplied with the overall voltage was made to the original current with moderate success. It was found that the precise value of shunt resistance is very sensitive to the deviation of measured ohmic resistance. We speculate that deviations of measured ohmic

Table 2
Numerical values of I-V and derivative characteristics of Schottky diode 1N5817.

Si schottky	V_m (V)[a]	V_o (V), γ = 2/3[b]	V_o (V), γ = 1/2[c]	V_t (V)[d]	$1/R_s$ (measured)[e]	dI/dV[f]	d^2I/dV^2 [g]	I_m (mA)[h]	I_m-cal (mA)[i]	Deviation (%)[j]	n (ideality factor)[k]
00	0.285	0.285	0.315	0.28	2.064	0.688	11.8	26.96	26.74	−0.813	1.00
60	0.220	0.225	0.255	0.24	0.176	0.059	1.025	2.22	2.25	1.278	0.99
120	0.210	0.205	0.235	0.23	0.101	0.034	0.532	1.36	1.42	4.439	1.09
180	0.195	0.195	0.225	0.22	0.065	0.022	0.365	0.851	0.856	0.597	1.02

[a,d,e,f,g,h,i,j,k]The definitions of these columns are listed in the caption of Table 1.

[b,c]V_o indicates the voltage at the minimum of Norde’s function, F(V), with different slope constant, γ. The second and the third column, $V_o(\gamma = 2/3)$ and $V_o(\gamma = 1/2)$, are the voltage at the minimum of F(V) with slope constant 2/3 and 1/2 respectively.

Table 3
Numerical values of I-V and derivative characteristics of lab-made Schottky diodes of concentric Al pads on p-type silicon.

Radius (μm)[a]	V_m(V)/I_m (μA)[b]	V_0 (V), γ = 1/2[c]	V_0 (V), γ = 2/3[d]	R_0, Norde[e]	R_s[f]	R_s/R_p/Leakage (%)[g]	R_{sub}/R_p/Leakage (%)[h]	$R_s/R_{sub}/R_p$/Leakage (%)[i]	n (ideality factor)[j]
100	0.14/46.9	0.17	0.14	277	272	275/31840/8.52	282/27780/9.74	269/13/26620/10.22	0.95
150	0.14/90.9	0.17	0.13	151	152	155/17330/8.01	157/17230/8.05	144/10/18520/7.55	1.09
200	0.11/103.5	0.14	0.11	129	127	128/12540/7.45	131/14130/6.59	114/14/13670/6.94	1.04
250	0.11/120.6	0.14	0.1	113	112	114/10760/7.41	116/13360/5.96	100/14/12220/6.64	1.08

[a]The radius of the central pad varies from 100 μm to 250 μm.
[b,c,d]The definitions of these columns are listed in the caption of Tables 1 and 2.
[e]R_o is the series resistance calculated from Norde's function.
[f]The R_s only is series resistance calculated in the situation of negligible shunt leakage and substrate resistance ($G_p = 0$, $R_{sub} = 0$).
[g]The R_s/R_p is the series resistance, shunt resistance in the assumption of $G_p \neq 0$, $R_{sub} = 0$.
[h]The R_{sub}/R_p is the substrate resistance, shunt resistance in the assumption of $G_p \neq 0$, $R_s = 0$.
[i]$R_s/R_{sub}/R_p$ considers the most complicated case, $G_p \neq 0$, $R_{sub} \neq 0$. The resistance is in the unit of ohm.
[g,h,i]Leakage (%) = I_p/I_m, which represents the ratio of shunt leakage current to the total diode current at V_m.
[j]The definition of j-th column is listed in the caption of Table 1.

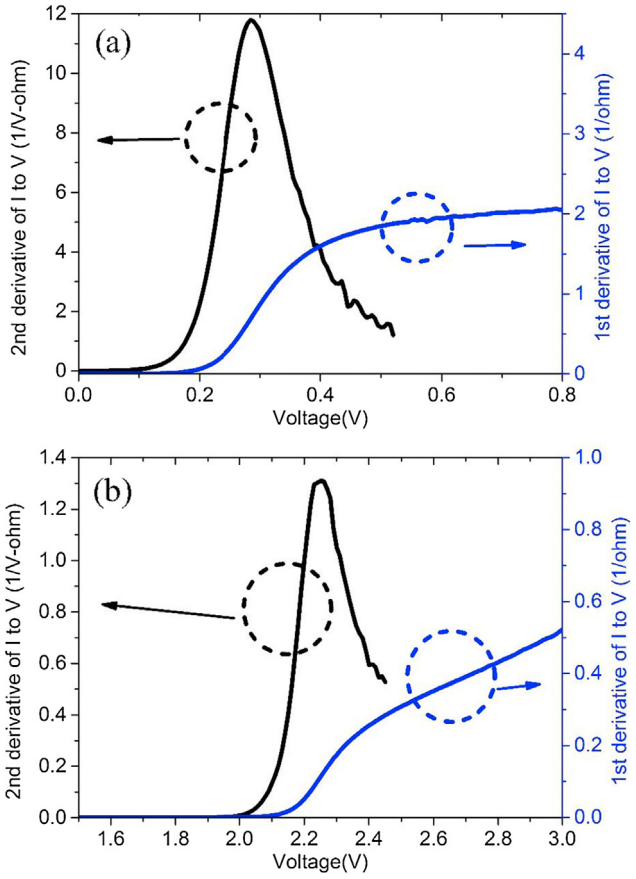

Fig. 4. Anomaly in dI/dV of diodes; (a) Typical diodes show plateauing dI/dV at high voltages, Diode A, but (b) some show another linear-like up-rise suggesting the current-voltage dependence is no longer linear but parabolic in Diode F.

resistance arise from the simplified circuit model since resistance associated with the bulk substrate is also a significant part of the total series resistance.

We have made in the lab Schottky diodes (Diode J in Table 1) with concentric aluminum pads having various radii in the central one against a fixed die of 5mmx5mm in p-type silicon. The radius of the central pad varies from 100 μm to 250 μm and the central pad is at a fixed 30 μm radially away from the outer pad. While the smaller central circle acts as the regular forward-biased Schottky diode the outer one is used as a leaky reverse-biased ohmic contact. Table 3 lists all numerical values of measured V_m, I_m and simulated R_{sub}, R_p and R_s in addition to R_o determined by Norde plot with a slope constant γ = 2/3. It is worthy to note that the measured R_o or sum of R_{sub} and R_s actually increases with decreasing radius of the central pads while the measured V_m or V_o increases. This is in sharp contrast to the trend noted in Table 2 where V_o or V_m decreases with an increasing external series resistance. In fact, an increasing series resistance would start to affect and regulate the output diode current in an ohmic manner at smaller applied voltage. For all diodes listed in Table 3 the dimension of the outer pad is pretty much fixed while the dimension of the central circle changes in radius. Since the outer pad is reverse biased the net current it can supply for the forward-biased central pad is limited by the area of the large outer pad which is limited in size. As the central pad increases in radius the fixed-size outer pad is actually acting as a relatively resistive load and one would expect a reduced turning point in the I-V curve, i.e. a smaller V_o by the Norde plot or V_m in the DIV approach. On the other hand, with an expanded radius in the central pad, the physical resistance actually decreases with an increasing cross section so it appears the parasitic resistance decreases accompanying with a seemingly decreasing "turn-on" voltage. Detailed numerical fitting also shows that the ratio of shunt leakage current, I_p, to diode current I_m, becomes larger as the central pad decreases in size, i.e. the percentage of leakage becomes more significant. Such a dependence on the pad radius is expected since the total diode current consists of the leakage part and a bulk component, which should be proportional to the pad area (square of radius). However, the shunt leakage should largely depend on the dimension of the gap region, if not properly passivated, between two concentric pads, and the gap area is proportional to the circumference of the pad. Therefore, the fraction of shunt leakage to the bulk component of the total diode current would decrease with the pad radius. Data corresponding to the scenario of R_{sub}/R_p (h-th column) in Table 3 yield the best fit to 1/radius with a coefficient of determination of 98.1%.

3.4. Voltage-dependent resistance

As mentioned in Norde's original report, the modified I-V plot of F (V) cannot tell the difference between a regular series resistance and that induced by a reverse-biased Schottky contact used to serve as an ohmic contact in the overall current circuit. The DIV approach may provide a glimpse on this issue since dI/dV actually manifests the change of current conduction. Some of the diodes measured have shown anomalies of another "turn-on" in the higher-voltage end of their dI/dV curve as shown in Fig. 4(b) instead of asymptotically becoming horizontal in Fig. 4(a). The up-rising trend indicates that the overall parasitic resistance actually begins to reduce with further applied voltage. We speculate the origin of this second "turn-on" in conductance comes from the quasi-ohmic contact based on reverse-biased Schottky

contact since the reverse I-V dependence of quasi-ohmic Schottky contact changes nonlinearly from low to high current with voltage, i.e. $dR_s/dV = 0$ is no longer valid. For a good ohmic contact, one would expect the I-V dependence to retain its linearity from low to high current. It is, however, beyond the scope of this work and it is worthy to be further investigated.

4. Conclusion

In summary, we have demonstrated with experimental results that higher order derivatives of conventional I-V measurements provide a simple access to determination of turn-on voltage, parasitic resistance and ideality factor of diodes. The methodology is simple with a self-consistency check better than 10% to about 1% for higher-resolution I-V characteristics. The peak voltage corresponding to the second derivative represents a turning point below which the conventional semi logarithmic I-V plot appears "linear". Above the turning point, the Log I-V plot is hampered by the parasitic resistance although the ideality factor may not have changed at all. The resistance-sensitive peak voltage of interest decreases with increasing parasitic resistance. The DIV approach matches with a special case of the well-known Norde plot for a specific slope constant. Yet, the general Norde approach provides additional measurable quantities complementary to the DIV approach. When both techniques are integrated to form a new analytical tool for diodes, it makes the diode modeling possible on quantitatively assessing not only the paracitic series resistance but also the often neglected shunt leakage.

Acknowledgements

This work has been financially supported by the Ministry of Science and Technology, Taiwan, through Grant No. 105-2221-E-007-005 and 106-2622-E-007-002-CC2. We gratefully acknowledge facility support from the Center for Nanotechnology, Materials Science and Microsystems of the National Tsing Hua University.

Appendix A

The relationship among R_s, R_{sub} and R_p is listed as follows:

$$A R_p^2 + B R_p + C = 0$$

where $A = (R_m - 3R_s - 3R_{sub})$, $B = (4R_mR_{sub} - 6R_sR_{sub} + 2R_mR_s - 2R_s^2 - R_{sub}^2)$, and $C = R_{sub}(R_mR_{sub} + 2R_mR_s - 2R_s^2 - R_sR_{sub})$ and the solution of R_p turns out to be:

$$R_p = \frac{-B \pm \sqrt{B^2-4AC}}{2A} \cong \frac{-B}{A} = \frac{4R_mR_{sub}-6R_sR_{sub} + 2R_mR_s-2R_s^2-R_{sub}^2}{3R_s + 3R_{sub}-R_m} \quad (9'')$$

Out of the two possible roots, the "negative" sign between $\pm$ would be chosen as one can find an unlikely solution of $R_p = 0$ for $R_{sub} = 0$ if the "plus" sign is chosen. Furthermore, the 4AC term is usually much smaller than B^2 and can be neglected for simplified calculation. Meanwhile, Eq. (5″) becomes an 8th-degree function of R_s:

$$\sum_{i=0}^{8} (\mathrm{CRSi}) R_s^i = 0 \quad (10'')$$

where the coefficient of R_s to the 8th power (CRS8) and the rest are:

$$\mathrm{CRS8} = [-4320Q_mR_mI_mR_{sub} + 1152Q_mR_m^2I_m - 16]$$

$$\mathrm{CRS7} = [280Q_mR_m^3I_m + 1296Q_mR_m^2I_mR_{sub} + 11592Q_mR_mI_mR_{sub}^2 - 1440Q_mR_mV_mR_{sub} - 336R_m + 520R_{sub}]$$

$$\mathrm{CRS6} = [-448Q_mR_m^3I_mR_{sub} + 2916Q_mR_m^2I_mR_{sub}^2 - 13647Q_mR_mI_mR_{sub}^3 - 8Q_mR_m^3V_m - 432Q_mR_m^2V_mR_{sub} + 846Q_mR_mV_mR_{sub}^2 + 112R_m^2 - 88R_mR_{sub} - 408R_{sub}^2]$$

$$\mathrm{CRS5} = [-16Q_mR_m^5I_m - 800Q_mR_m^4I_mR_{sub} + 360Q_mR_m^3I_mR_{sub}^2 + 14724Q_mR_m^2I_mR_{sub}^3 - 5493Q_mR_mI_mR_{sub}^4 - 128Q_mR_m^4V_m + 1860Q_mR_m^3V_mR_{sub} - 684Q_mR_m^2V_mR_{sub}^2 + 10701Q_mR_mV_mR_{sub}^3 - 124R_m^3 + 832R_m^2R_{sub} - 144R_mR_{sub}^2 - 792R_{sub}^3]$$

$$\mathrm{CRS4} = [384Q_mR_m^5I_mR_{sub} - 3156Q_mR_m^4I_mR_{sub}^2 + 7914Q_mR_m^3I_mR_{sub}^3 + 8037Q_mR_m^2I_mR_{sub}^4 + 2998Q_mR_mI_mR_{sub}^5 + 32Q_mR_m^5V_m - 1264Q_mR_m^4V_mR_{sub} + 7152Q_mR_m^3V_mR_{sub}^2 - 8208Q_mR_m^2V_mR_{sub}^3 + 4545Q_mR_mV_mR_{sub}^4 + 80R_m^4 - 913R_m^3R_{sub} + 1056R_m^2R_{sub}^2 - 1280R_mR_{sub}^3 - 948R_{sub}^4]$$

$$\mathrm{CRS3} = [1770Q_mR_m^5I_mR_{sub}^2 - 9796Q_mR_m^4I_mR_{sub}^3 + 14911Q_mR_m^3I_mR_{sub}^4 - 6426Q_mR_m^2I_mR_{sub}^5 - 81Q_mR_mI_mR_{sub}^6 + 256Q_mR_m^5V_mR_{sub} - 4508Q_mR_m^4V_mR_{sub}^2 + 12990Q_mR_m^3V_mR_{sub}^3 - 8937Q_mR_m^2V_mR_{sub}^4 - 927Q_mR_mV_mR_{sub}^5 - 16R_m^5 + 456R_m^4R_{sub} - 1488R_m^3R_{sub}^2 - 1280R_m^2R_{sub}^3 + 2580R_mR_{sub}^4 + 18R_{sub}^5]$$

$$\mathrm{CRS2} = [3917Q_mR_m^5I_mR_{sub}^3 - 12541Q_mR_m^4I_mR_{sub}^4 + 4812Q_mR_m^3I_mR_{sub}^5 + 7974Q_mR_m^2I_mR_{sub}^6 - 4725Q_mR_mI_mR_{sub}^7 + 773Q_mR_m^5V_mR_{sub}^2 - 8356Q_mR_m^4V_mR_{sub}^3 + 18555Q_mR_m^3V_mR_{sub}^4 - 14643Q_mR_m^2V_mR_{sub}^5 + 3348Q_mR_mV_mR_{sub}^6 - 88R_m^5R_{sub} + 824R_m^4R_{sub}^2 - 360R_m^3R_{sub}^3 - 2460R_m^2R_{sub}^4 + 246R_mR_{sub}^5 + 494R_{sub}^6]$$

$$\mathrm{CRS1} = [4312Q_mR_m^5I_mR_{sub}^4 - 7986Q_mR_m^4I_mR_{sub}^5 + 2519Q_mR_m^3I_mR_{sub}^6 - 198Q_mR_m^2I_mR_{sub}^7 + 957Q_mR_m^5V_mR_{sub}^3 - 5687Q_mR_m^4V_mR_{sub}^4 + 4653Q_mR_m^3V_mR_{sub}^5 - 594Q_mR_m^2V_mR_{sub}^6 - 160R_m^5R_{sub}^2 + 608R_m^4R_{sub}^3 + 940R_m^3R_{sub}^4 - 338R_m^2R_{sub}^5 - 196R_mR_{sub}^6 + 54R_{sub}^7]$$

$$\mathrm{CRS0} = [1936Q_mR_m^5I_mR_{sub}^5 - 968Q_mR_m^4I_mR_{sub}^6 + 121Q_mR_m^3I_mR_{sub}^7 + 484Q_mR_m^5V_mR_{sub}^4 - 1573Q_mR_m^4V_mR_{sub}^5 + 363Q_mR_m^3V_mR_{sub}^6 + 27Q_mR_mV_mR_{sub}^8 - 96R_m^5R_{sub}^3 - 112R_m^4R_{sub}^4 + 106R_m^3R_{sub}^5 + 38R_m^2R_{sub}^6 - 30R_mR_{sub}^7 + 4R_{sub}^8]$$

Appendix B. Supplementary material

Supplementary data associated with this article can be found, in the online version, at https://doi.org/10.1016/j.sse.2018.08.002.

References

[1] Sah CT, Noyce RN, Shockley W. Carrier generation and recombination in P-N junctions and P-N junction characteristics. Proc IRE 1957;45:1228–43. https://doi.org/10.1109/JRPROC.1957.278528.

[2] Sze SM, Coleman DJ, Loya A. Current transport in metal-semiconductor-metal (MSM) structures. Solid State Electron 1971;14:1209–18. https://doi.org/10.1016/0038-1101(71)90109-2.

[3] Norde H. A modified forward I-V plot for Schottky diodes with high series resistance. J Appl Phys 1979;50:5052–3. https://doi.org/10.1063/1.325607.

[4] Bohlin KE. Generalized Norde plot including determination of the ideality factor. J Appl Phys 1986;60:1223–4. https://doi.org/10.1063/1.337372.

[5] Lien CD, So FCT, Nicolet MA. An improved forward I-V method for nonideal Schottky diodes with high series resistance. IEEE Trans Electron Devices 1984;31:1502–3. https://doi.org/10.1109/T-ED.1984.21739.

[6] Cibils RM, Buitrago RH. Forward I-V plot for nonideal Schottky diodes with high series resistance. J Appl Phys 1985;58:1075–7. https://doi.org/10.1063/1.336222.

[7] Werner JH. Schottky barrier and pn-junction I/V plots - Small signal evaluation. Appl Phys A Solids Surf 1988;47:291–300. https://doi.org/10.1007/BF00615935.

Wei-Fu Wang received his B.S. degree in Electrical Engineering from National Tsing Hua University, Taiwan in 2012, where he is currently pursuing the Ph.D. degree under the advise of Prof. K.C. Hsieh with the Institute of Electronics Engineering. His research interests include impurity induced disordering for high-power -808nm laser diode and material analysis.

Kai-Yuan Cheng received his B.S. (2008) and M.S. (2010) degrees in Material Sciences and Engineering from National Tsing Hua University, Taiwan. He is currently pursuing the Ph.D. degree at Institute of Electronics Engineering, National Tsing Hua University under the tutelage of Prof. K.C. Hsieh. His research interests include GaN- based devices, material analysis and their applications in future electronics.

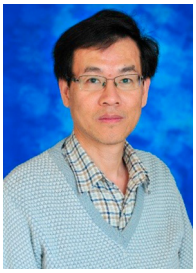

Meng-Chyi Wu received the Ph.D. degree in electrical engineering from National Cheng Kung University, Taiwan, in 1986. He has over 30 years of research experience on III–V compound semiconductors, material characterization, optoelectronic devices, and epitaxial techniques consisting of liquid-phase epitaxy, metalorganic chemical vapor deposition (MOCVD), and molecular-beam epitaxy. He currently a Faculty member with Institute of Electronic Engineering, National Tsing Hua University in Taiwan.

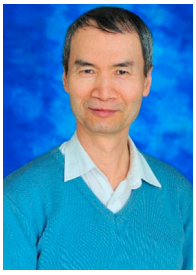

Kuang-Chien Hsieh received the Ph.D. degree in materials science and engineering from the University of Illinois at Urbana–Champaign, Champaign, IL, USA, in 1982. He was a Faculty Member with the Department of Electrical and Computer Engineering, University of Illinois, from 1987 to 2010. He was a professor in the Institute of Electronics Engineering and also the Director of the Center for Nanotechnology, Microsystems and Materials Science with National Tsing Hua University, Hsinchu, Taiwan from 2010 to 2017. Afterwards, he retired from the Institute of Electronics Engineering, National Tsing Hua University in 2017. His research mainly focuses on compound semiconductor epitaxy, material analysis and solid-state physics.